A Friction and Adhesion Characterization Setup for Extreme Temperatures

by

Sunil Mate

A Thesis Presented in Partial Fulfillment
of the Requirements for the Degree
Master of Science

Approved April 2016 by the
Graduate Supervisory Committee:

Hamidreza Marvi, Chair
Konrad Rykaczewski
Hyunglae Lee

ARIZONA STATE UNIVERSITY

May 2016

ABSTRACT

It is well known that the geckos can cling to almost any surface using highly dense micro/nano fibrils found on the feet that rely on Van Der Waals forces to adhere. A few experimental and theoretical approaches have been taken to understand the adhesion mechanism of gecko feet. This work explains the building procedure of custom experimental setup to test the adhesion force over a temperature range and extends its application in space environment, potentially unsafe working condition.

This study demonstrates that these adhesive capable of switching adhesive properties not only at room environment but also over a temperature range of -160^{o}C to 120^{o}C in vacuum conditions. These conditions are similar to the condition experienced by a satellite in a space orbiting around the earth. Also, this study demonstrated various detachment and specimen patch preparation methods. The custom-made experimental setup for adhesion test can measure adhesion force in temperature and pressure controlled environment over specimen size of 1 sq. inch. A cryogenic cooling system with liquid nitrogen is used to achieve -160^{o}C and an electric resistive heating system are used to achieve 120^{o}C in controlled volume. Thermal electrodes, infrared thermopile detectors are used to record temperature at sample and pressure indicator to record vacuum condition in controlled volume. Reversibility of the switching behaviour of the specimen in controlled environment confirms its application in space and very high or very low-temperature conditions.

The experimental setup was developed using SolidWorks as a design tool, Ansys as simulation tool and the data acquisition utilizes LabVIEW available in the market today.

DEDICATION

I dedicate all this hard work to my parents, Munjaji and Anusuya Mate, for their truly unconditional love and long distance support. I would also like to dedicate this work to my sister and dear friend, Ashwini Rode and Nitesh Mule, for being people to look up to.

ACKNOWLEDGMENTS

I would like to thank Dr. Hamidreza Marvi for his invaluable advice, guidance and support that made this work possible and with whom it has been a true privilege to work with. In addition to giving me this golden opportunity to research exactly what I wanted, he has also helped me grow as a researcher and person.

I would like to thank Dr.Owen Hildreth and Dr. Konrad Rykaczewski for making available time in their laboratory courses for my research experiment. I would also like to thank Dr.Hyunglae Lee and Dr. Konrad Rykaczewski for taking their time to serve as my thesis committee members. Lastly, I would like to thank my family and friends for their after-hours support and motivation.

TABLE OF CONTENTS

LIST OF TABLES

LIST OF FIGURES

Chapter 1

INTRODUCTION

1.1 Project Purpose and Need

Gecko has the most complex, efficient and versatile attachment system which enables them to attach quickly and reversibly to surfaces of varying chemistry and topography, i.e. smooth and rough surfaces,(Autumn *et al.*, 2002). As shown in Figure 1, their feet are covered with millions of fine fibrils or setae, which play a crucial role in adhesion to surfaces, (Jagota and Bennison, 2002). Each 30-130 μm long setae is only one-tenth the diameter of a human hair and contains hundreds of projections terminating in 0.2 -0.5 μm spatula-shaped structures,(Russell, 2002; Ruibal and Ernst, 1965).

Geckos are the largest known animals with hairy attachment pads, (Autumn *et al.*, 2000, 2002). Their attachment system is a "dry" system and does not rely on adhesion enhancing secretions. Although some phospholipids were found in gecko footprints,(Hsu *et al.*, 2011) the function of these lipids seems to be irrelevant for adhesion. The adhesive interaction of gecko toe pads with a surface is mainly based on van der Waals forces,(Autumn *et al.*, 2002) likely enhanced by capillary forces due to humidity,(Buhl *et al.*, 2009; Huber *et al.*, 2007). Geckos can generate large forces, reaching surprisingly high shear strength of up to 100kPa,(Autumn *et al.*, 2000). Detachment is controlled by the anisotropy of the adhesive structures and the biomechanics of the gecko's motion, which consists of simultaneous shear and peel movement,(Autumn *et al.*, 2006).

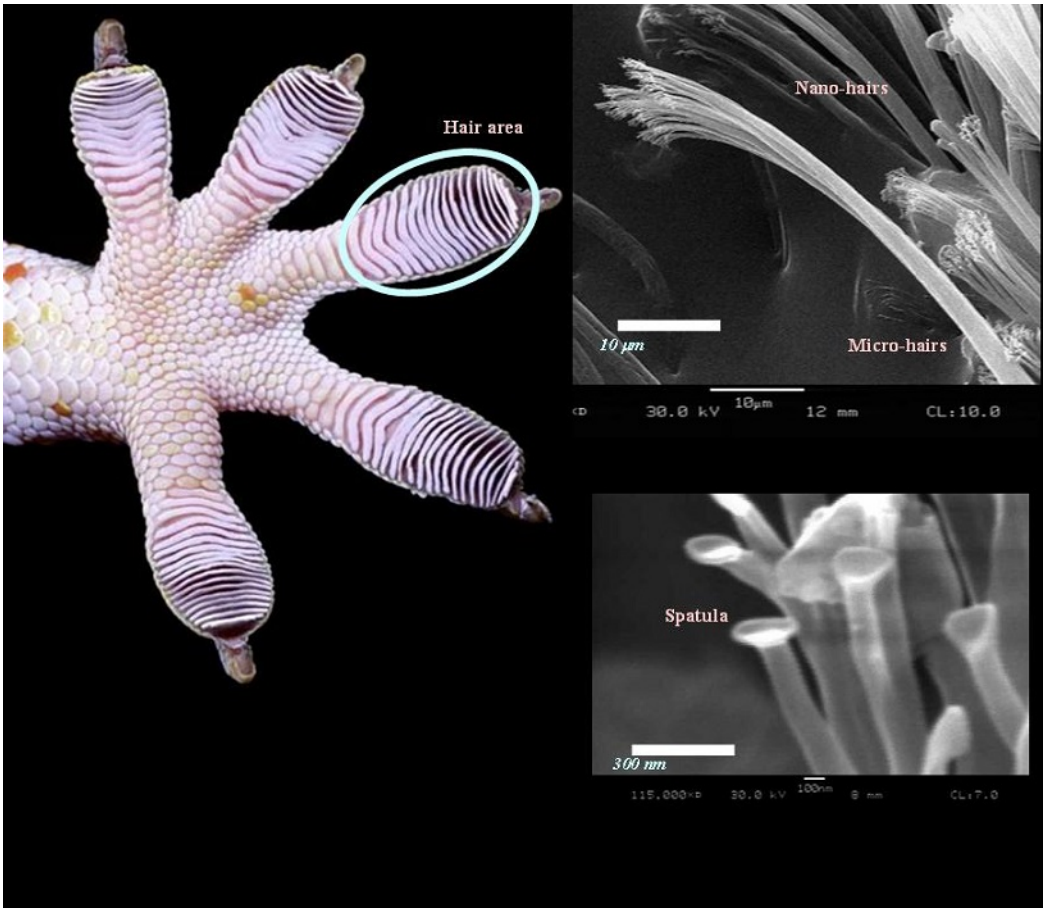

Figure 1: Gecko foot and setae seen through electronic microscopy

Source: Anitei (2007)

High adhesive forces, quick and easy detachment, dry "residue free" contact and operational in the extreme environment are the properties of the gecko's adhesion system. As shown in Table 1, these characteristics are superior to those of many other temporary attachment mechanisms found in nature. Thus, it is not surprising that this attachment system gains growing attention, not only from the scientific community but also from industry, especially as its properties may lead to new artificial attachment devices, which could replace the traditional energy consuming, noisy attachment systems. Artificial bio-inspired adhesive systems have been extensively studied,(Kamperman

	Animals	Substrate Types & Environmental Conditions	Controllability	Dirt Resistance	Substrate Damage or Residue	Power Efficiency	Speed
Mechanical Interlocking	plants, insects, monkeys, squirrels, ...	Soft penetrable and very rough rigid surfaces; Air, liquid, vacuum	Low	High	High damage	Medium	Low
Vacuum Suction	octopus, salamander, ...	Smooth surfaces (with no pores & cracks)	High	Medium	Possible damage to tissue, etc.	Low	Low
Wet Fibrillar Structure	muscles, ants, cockroaches, frogs, crickets, ...	Surfaces that can wet the liquid secretion	Medium	Medium	No damage but some liquid residue	Medium	Medium
Dry Fibrillar Structure	geckos, spider, kissing bug, ...	Almost any smooth or micron scale rough surface	Medium	Medium	No damage or residue	High	High

Table 1: Temporary attachment mechanisms in nature
Gorb (2008)

et al., 2010; Heepe and Gorb, 2014; Pattantyus-Abraham *et al.*, 2013; Sameoto and Menon, 2010; Zhou *et al.*, 2013) and comparably high adhesive performance was reached, even exceeding the so-called "gecko limit" of 100 kPa,(Del Campo *et al.*, 2007).

Besides fabrication and characterization of bio-inspired adhesive with high and robust adhesion and adhesion control using "passive" peeling or shearing, the control of adhesion by an external stimulus has been studied (Arul and Ghatak, 2012; Kier and Smith, 2002; Jeong *et al.*, 2010; Kim *et al.*, 2009; Nadermann *et al.*, 2010) and improved to obtain switchable adhesive even in extreme environment like outer space, (Henrey *et al.*, 2013).

1.2 Goals

In addition, the effects of environmental conditions such as humidity, pressure and temperature on adhesion have been investigated in a few studies. While gecko adhesion has been shown to depend on ambient humidity (Henrey *et al.*, 2013), adhesion of synthetic dry adhesive made from Polydimethylsiloxane (PDMS) is not affected by humidity. The adhesion of PDMS is robust to reduction in the ambient pressure down to 10^{-5} mbar, as well as temperature changes between -50^{o}C and 75^{o}C, even though the stiffness (effective Young's Modulus) of the material underwent changes (linearly with temperature),(Henrey *et al.*, 2013; Jiang *et al.*, 2015). Although there are a few studies on the effect of temperature on adhesion (Henrey *et al.*, 2013; Ruffatto *et al.*, 2014; Jiang *et al.*, 2015; Feldstein *et al.*, 2014; Gåård *et al.*, 2010; Loguercio *et al.*, 2011; Kim *et al.*, 2009), switchable adhesive under extreme temperatures and pressures are not much studied. Particularly, none of these few studies has explored the wide range of temperature experienced in space (e.g. -160^{o}C to 120^{o}C at the International Space Station). Such a wide temperature range will make the experimental study of fibrillar adhesive much more complex. The goal of this study was to design and fabricate a highly customized adhesion characterization system which works on a wide temperature range.

Chapter 2

ENVIRONMENTAL CHAMBER

In this study, the adhesive performance of a bio-inspired adhesive is tested both in the vacuum and extreme temperature range from -160^{o}C to 120^{o}C, similar to the environment condition faced by a satellite while orbiting around the earth in outer space (Price *et al.*, 2001) or work condition with extreme temperature conditions. These temperature and pressure conditions were the same design conditions used by NASA for designing satellites. A chamber of dimension 25cm (L) X 25cm (B) X 19cm (H) is designed to conduct experimental measurements inside the controlled environment. Acrylic plexiglass is used as a material for fabrication of chamber. It is fabricated to hold a vacuum and operate under the temperature range from -160^{o}C to 120^{o}C. One of the design consideration was that the chamber must be sealed and leave no obstruction to the vacuum. Edges of the chamber were chamfered with chamfer router for better sealing against vacuum.

2.1 Parametric Study for Chamber Wall Thickness

A parametric study has been done in ANSYS software to decide the wall thickness of chamber. A load of 1atm pressure is applied on wall face with fixed edges. According to parametric study shown in Figure 2 and Figure 3, the relative changes in total deformation and stress values against various wall thicknesses are comparably small after 10mm of wall thickness. Total deformation of 27 μm and equivalent stress of 11.25 MPa is observed when wall thickness set to 10mm. Total deformation and

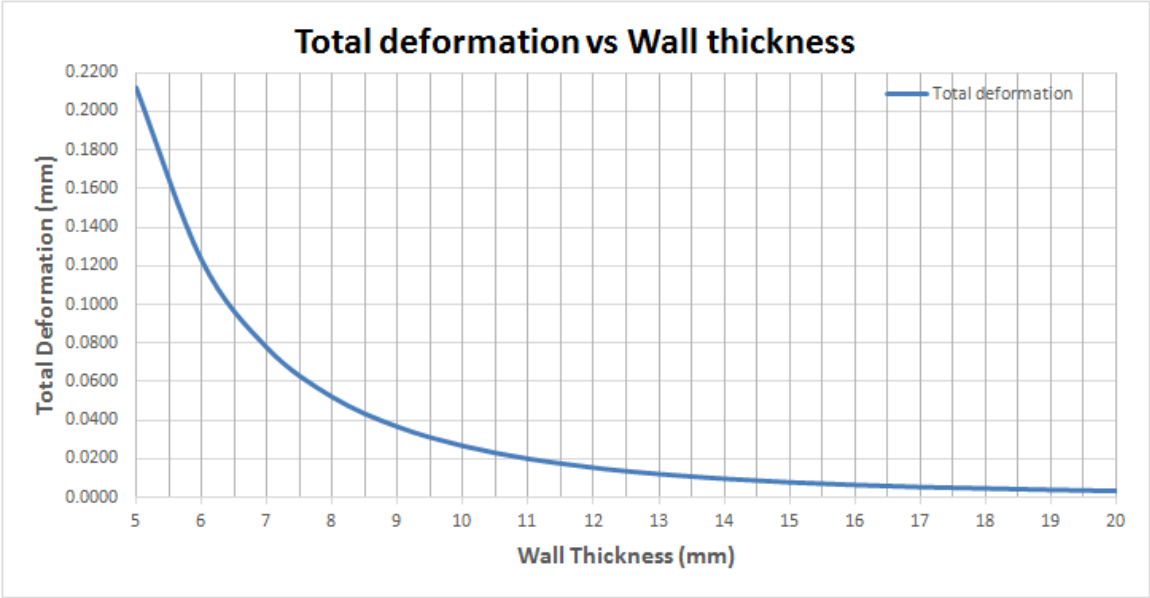

Figure 2: ANSYS parametric result for total deformation against wall thickness

equivalent stress at the wall thickness of 10mm is acceptable and in the safe limit for Acrylic material. To be on the safer side next high thickness value, 12.5 mm is selected for chamber fabrication. The total deformation and equivalent stress for 12.5 mm thick acrylic plexiglass are 14 μm and 7.24 MPa, respectively.

2.2 Chamber Top Face Fabrication

A hole of 70 mm in diameter was cut on the top face of the chamber using 75W Universal laser cutting machine. The hole on the top of the chamber is to allow the entrance of an indenter that will test the friction and adhesion force characteristics of the sample hold inside the chamber. Initially, a thick piece of rubber was used to cover the hole and assumed to be sufficient enough to seal the vacuum in the chamber and allow movement of the indenter. But the idea of a thick piece of rubber was scraped

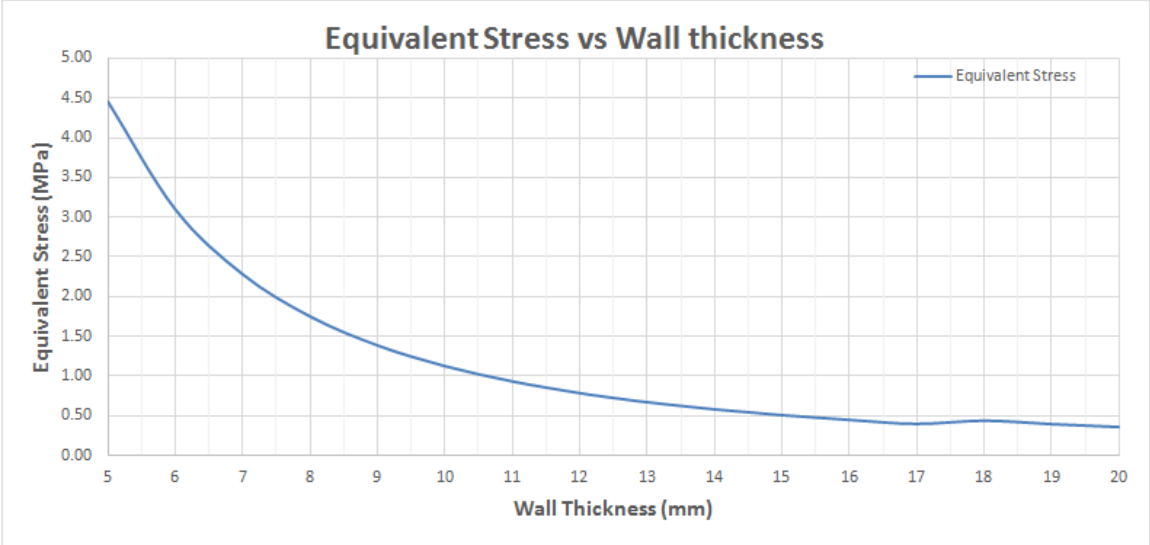

Figure 3: ANSYS parametric result for equivalent stress against wall thickness

as rubber piece found to be highly stiff to allow movement of the indenter. Then a thick piece of rubber was replaced by tapered rubber bellow or also known as dust cover. The schematic of Dust cover is shown in Figure 4. These are manufactured by McMaster-CARR Supplies, product no. 9744K17. The specifications for dust cover are summarized in Table 2. Dust cover is made of single dipped, molded, black neoprene and latex, which is flexible enough to allow movement of indenter in any direction up to 25 mm. The top flange of the dust cover is clamped between two rings shaped acrylic plexiglass with tapped holes for better sealing. The inner diameter of these rings matched and aligned with the hole on top of the chamber. Two rings were fixed and sealed on the top face of the chamber as shown in Figure 5.

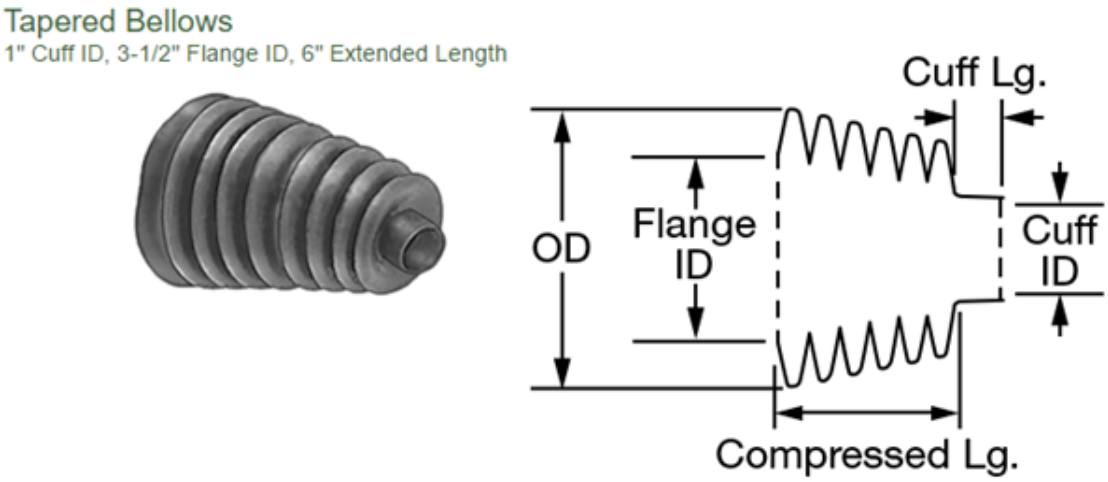

Figure 4: Schematic of tapered bellow

Product number	**9744K17**
Shape	Round
End type	One cuff end and one flange end
Cuff ID	1”
Cuff length	1”
Flange ID	3 ½”
OD	4 ¾”
Extended length	6”
Compressed length	1 ½"

Table 2: Specifications of tapered bellow

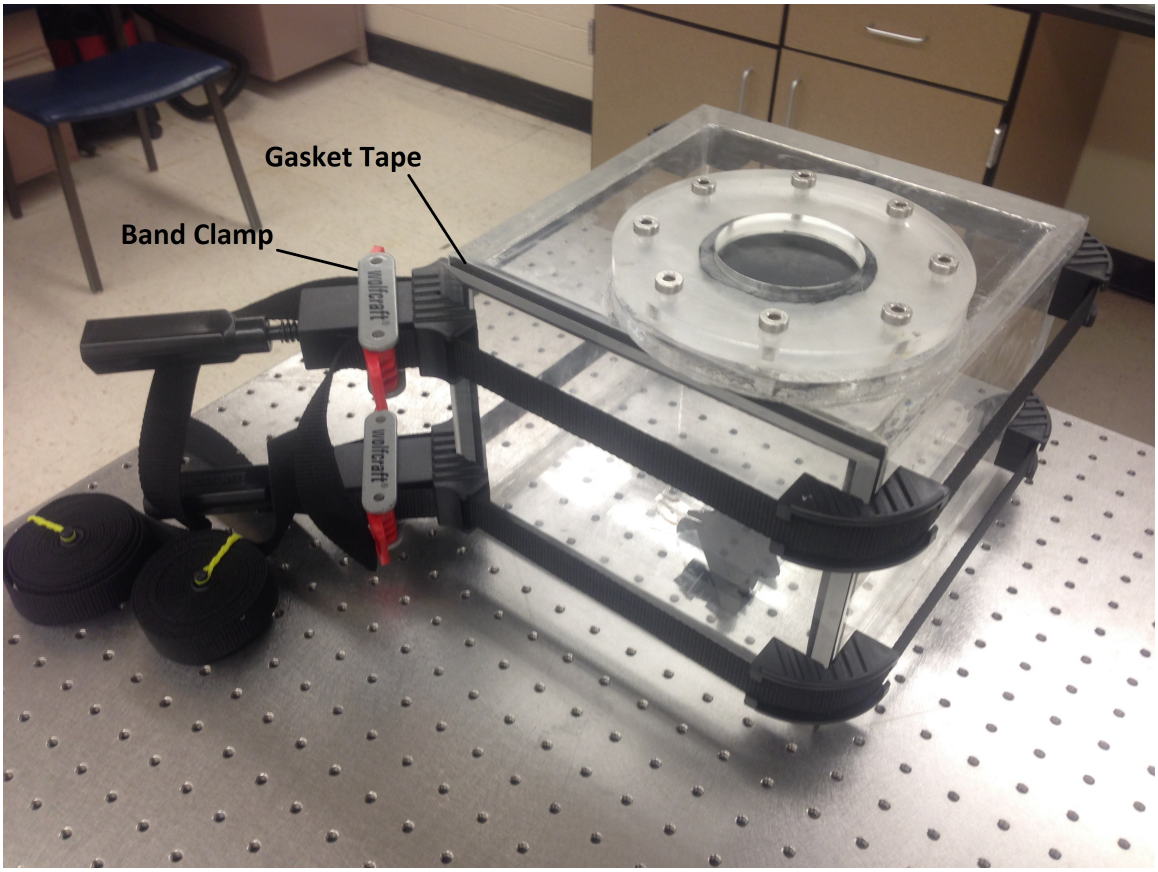

Figure 5: Environment controlled chamber with gasket tape and band clamp

2.3 Chamber Assembly

The chamfered edges of the chamber are glued together by using Weld-On 4 Acrylic adhesive, a product that welds together pieces of acrylic. Weld-On 4 is a liquid solvent which softens the edges of acrylic and weld two pieces of acrylic. After welding together the edges of the chamber, silicon used to insure perfect sealing by applying along the edges. The front face of the chamber is used as an access door to the inside of the chamber and it is not welded to the chamber. Whereas, it is sealed to the chamber by using gasket tape and a band clamp as shown in Figure 5.

Manual stages fixed inside the chamber using a small piece of acrylic and Weld-On 4. The sample to be tested is placed on Z shaped steel bracket, which is connected to manual stages. Linear movement and orientation of sample with respect to indenter are controlled by manual actuation of manual stages. The Z-shaped steel bracket is manufactured by machining of steel block. As machined steel bracket is more rigid than the bracket made by bending steel plate, the machining process is preferred over bending a steel plate to form Z shape bracket.

A turbo pump is installed next to chamber to remove all the air from controlled space of chamber and created the vacuum. The created vacuum is of order 10^{-5} mbar. A pressure sensor and PID (Proportional-Integral-Derivative) controller built in the turbo pump system is used for controlling the pressure of the chamber. The cryogenic cooling system used for lowering the temperature of the sample to -160^{o}C by allowing liquid nitrogen through copper tubing underneath the sample. Inert gasses introduced into the chamber periodically, in order to avoid freezing around cylindrical pillars of the sample. The electric resistive heating system used to reach 120^{o}C. A heating coil made of copper and placed around the sample. Infrared thermopiles are used for measuring the temperature of the sample. The flow of the liquid nitrogen is regulated using proportional valve and the voltage of the resistive heating element will be controlled by a PID controller to adjust the temperature at the desired value. Ceramic disk is used as thermally isolating element and placed below the cooling or heating stage to protect the electronics used in the setup and avoided wasting energy for heating or cooling.

The chamber is placed on a vibration isolator table since the measurements are very sensitive to any vibrations. The vibration isolator table from Newport supplies is active which uses a narrowband precision tunable damper to isolate vibrations as

Figure 6: Vibration isolator table

Model	Vertical Isolation			Horizontal Isolation		
	Resolution (Hz)	5Hz (%)	10Hz (%)	Resolution (Hz)	5Hz (%)	10Hz (%)
Integrity Isolator	1.5	88	98	1	88	98

Table 3: Isolation specification of vibration isolator table

showed in Figure 6. The isolation specifications of the table are summarized in Table 3. As per isolation specification of the table, it cancels the talking frequency which ranges from 85Hz - 250Hz and partially cancels walking frequency which ranges from 2Hz - 5Hz. The turbo pump and liquid nitrogen flow need to be shut down during the experimental measurements so as not to impose any vibration to the sample.

Chapter 3

FRICTION AND ADHESION CHARACTERIZATION SYSTE

3.1 Indenter Positioning Ssystem

The adhesion characterization system shown in Figure 10, consists of a linear X-Y-Z positioning system and a load cell. A single axis linear motorized actuator is shown in Figure 7a. A motorized linear X-Y-Z positioning system is build by using similar three single axes linear actuator along with a right angle bracket as shown in Figure 7b. The key specifications of a motorized linear actuator are summarized in Table 4. Position and speed of the indenter are controlled by motorized linear actuators while the position and orientation of sample are controlled by the combination of manual linear actuators and goniometer.

3.2 Sample Orientation and Positioning System

A single axis translational stage with a standard micrometer and a goniometer is shown in Figure 8a and Figure 8b respectively. The sample is placed on a glass slide, which is then attached to goniometer through the Z-shaped bracket. Lower flange end of the Z-Shaped bracket is fixed to the glass slide and upper flange end is connected to goniometer. This whole assembly along with goniometer is attached on manual linear actuators inside the chamber through custom manufactured adapter from a piece of acrylic. As shown in Figure 9, the goniometer is aligned at a 45^o with respect to the manual actuator to maximum use of space available to position sample

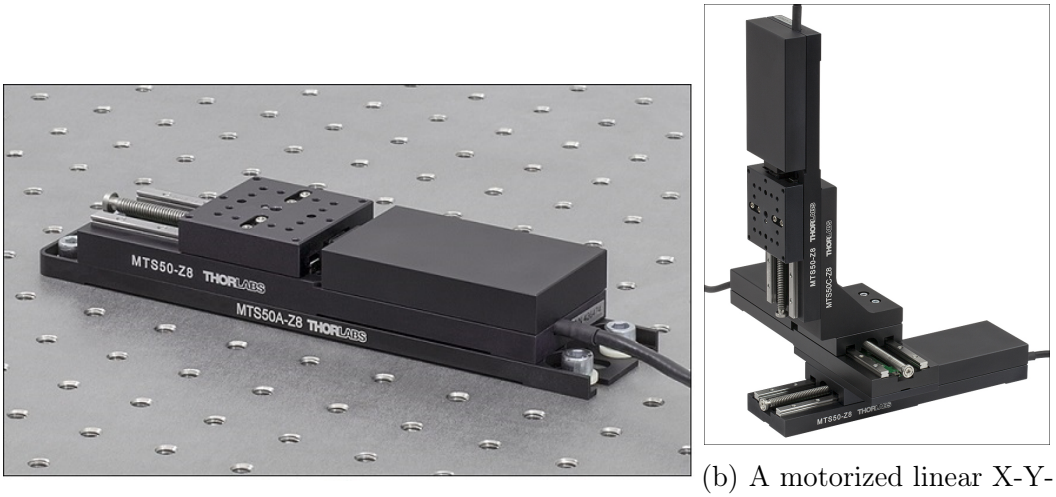

(a) A single axis motorized linear actuator

(b) A motorized linear X-Y-Z positioning system

Figure 7: Types of linear actuators

inside the chamber. Manual actuators are used for initial calibration before each set of experimental measurements.

3.3 Sample Imaging During Experiment

Motorized linear actuators can extend up to 50mm along X-Y-Z direction while manual linear actuators can extend up to 25mm in X-Y direction. Goniometer can orient sample up to $\pm 10^o$. Inverted microscope along with CMOS (Complementary metal-oxide semiconductor) camera is used to record the dynamic behavior of sample when indenter touches the sample. Magnification power of inverted microscope ranges from a minimum of 0.35X to maximum 2.25X and working distance varies from 45.6mm to 42.4mm respectively. In order to keep the sample within working distance of inverted microscope, the sample is lowered with the help of Z-shaped bracket. A

Product number	MTS50-Z8
Travel range	50 mm (1.97”)
Velocity (Max)	2.4 mm/s
Min. achievable incremental movement	0.05 µm
Backlash	<6 µm
Bidirectional repeatability	1.6 µm
Horizontal load capacity (Max)	25 lbs (12 Kg)
Vertical load capacity (Max)	10 lbs (4.5 Kg)
Included actuator	Build-In DC Servo

Table 4: Key specification of linear actuator

(a) A single axis translational manual stage with micrometer

(b) A goniometer

Figure 8: Orientation and positioning system

hole is cut on the lower flange of the Z-shaped bracket to view the sample from the bottom.

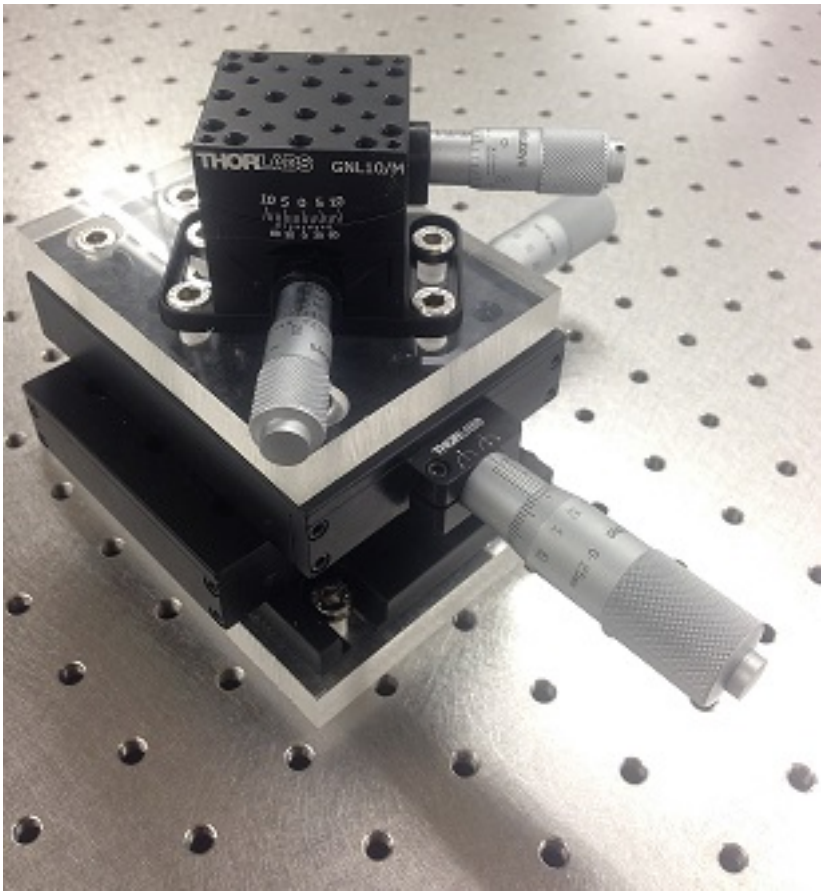

Figure 9: Assembly of goniometer and X-Y manual stages

A 6 axis load cell is used to record the adhesion and friction force exerted by the sample on indenter. One side of the load cell is connected to indenter whereas the other is connected to the motorized X-Y-Z actuator. Rubber bellow, also known as dust cover is used to seal connecting rod of indenter to Z axis motorized linear actuator as shown in Figure 10. Rubber bellows are flexible enough to allow indenter movement in X-Y-Z direction. Infrared thermopiles are used to measure the temperature of the sample. Ceramic connectors are used at two locations, one between indenter and load cell, and second below the glass slide. Ceramic connectors are used to avoid heat flow from cooling or heating system to the linear actuators and other electronic instruments.

Product number	PT1/M
Travel range	25 mm (1")
Min. achievable incremental movement	500 µm translation per revolution
Orthogonality	<5 mrad
Angular deviation	<250 µrad
Horizontal load capacity (Max)	90 lbs (41 Kg)
Vertical load capacity (Max)	20 lbs (9 Kg)
Included actuator	Micrometer (Manual)

Table 5: Common specifications of single axis translational stage

Product number	GNL20
Rotation range	±10°
Accuracy	10 arcmin (0.167°)
Load capacity	1 lb (0.45 Kg)

Table 6: Common specifications of goniometer

3.4 ANSYS Thermal Analysis of Environment Chamber

Thermal analysis of experimental chamber has been done to analyze the heat flow from heating and cooling stage to the other surrounding components. A transient thermal analysis is done in ANSYS software. The transient thermal study is performed with two extreme thermal loading conditions. One being set to -160^{o}C and simulation ran to get heat distribution over Z-shaped bracket and indenter. The same simulation ran with other extreme thermal condition set to 120^{o}C. Conduction and radiation are

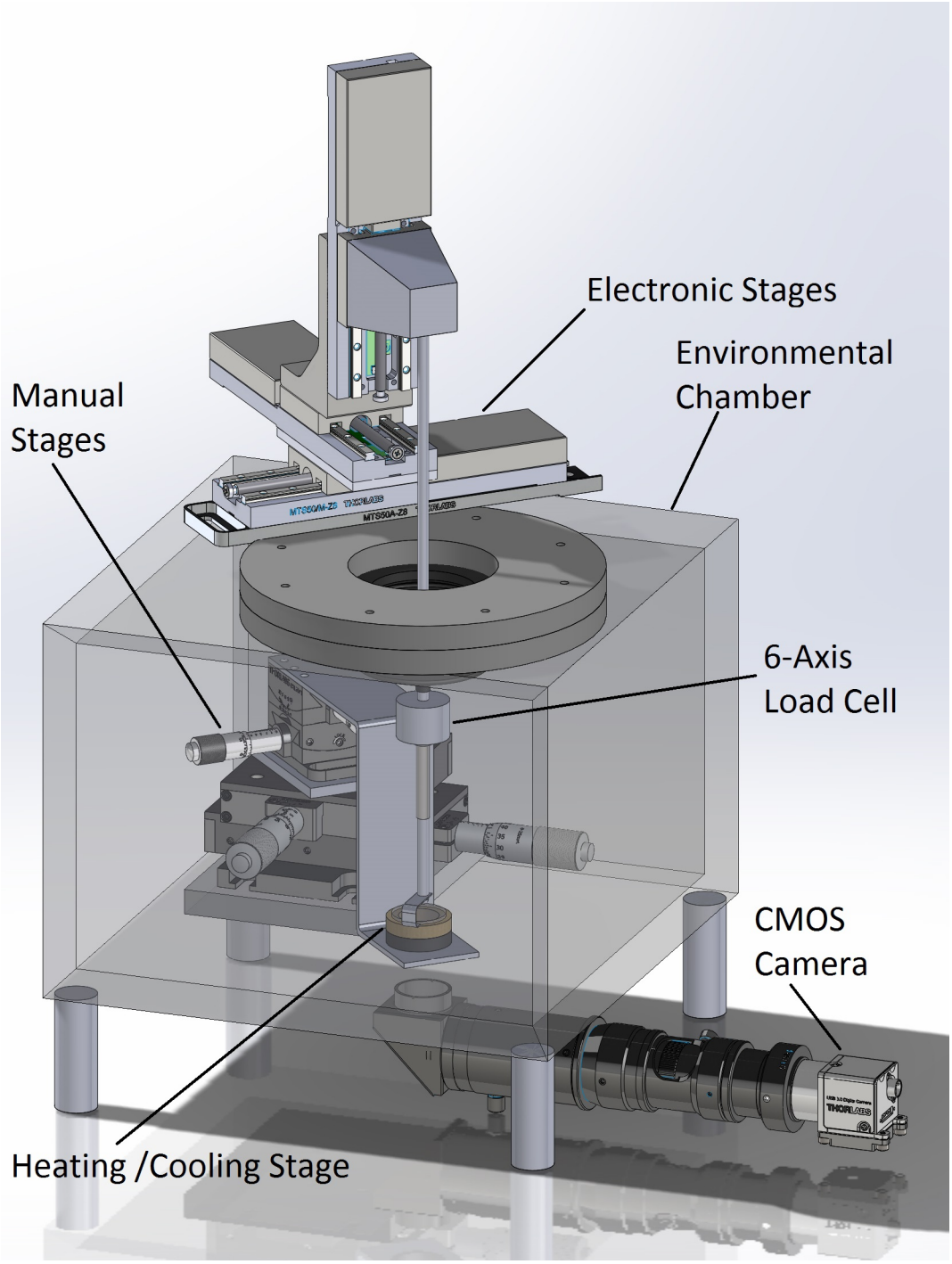

Figure 10: Schematic of adhesion characterization experimental setup and environmental chamber

Vacuum range	Pressure in hPa (mbar)	Pressure in mmHg (Torr)	Molecules / m^3	Mean free path
Ambient pressure	1013	759.8	2.7×10^{25}	68 nm
Low vacuum	300 - 1	225 - 7.501×10^{-1}	10^{25} - 10^{22}	0.1 - 100 μm
Medium vacuum	1 - 10^{-3}	7.501×10^{-1} - 7.501×10^{-4}	10^{22} - 10^{19}	0.1 - 100 mm
High vacuum	10^{-3} - 10^{-7}	7.501×10^{-4} - 7.501×10^{-8}	10^{19} - 10^{15}	10 cm - 1 Km
Ultra high vacuum	10^{-7} - 10^{-12}	7.501×10^{-8} - 7.501×10^{-13}	10^{15} - 10^{10}	1 Km - 10^5 Km
Extremely high vacuum	$<10^{-12}$	$<7.501 \times 10^{-13}$	$<10^{10}$	$> 10^5$ Km

Table 7: Typical values for air at different pressures
Wikipedia (2016)

the heat transfer phenomenon considered during the whole simulation run. Convection is ignored during ANSYS simulation as the whole experiment is carried out in low pressure 10^{-5} mbar, which falls in the category of high vacuum according to Table 7.

From Table 7, it can be deduced that the mean free path for air molecules ranges from 10 cm – 1Km for pressure 10^{-5} mbar. This means that for pressure 10^{-5} mbar, air molecules have to travel a distance which ranges from 10 cm to 1 Km, to effectively transfer energy between successive impacts. For environment chamber which is a rectangular prism with dimension 25cm X 25cm X 19cm, the value of the mean free path is very large and thus possibility of convection heat transfer can be ignored.

3.4.1 Thermal Analysis for Extreme Low Temperature

Initially, thermal analysis for extreme low temperature is carried out. The cooling stage is set to temperature of -160^{o}C and end step of transient thermal analysis set to 3600 sec. A 24 gauge copper strip is attached to the cooling stage and another end is connected to indenter tip. Indenter tip is allowed to pass through a punched

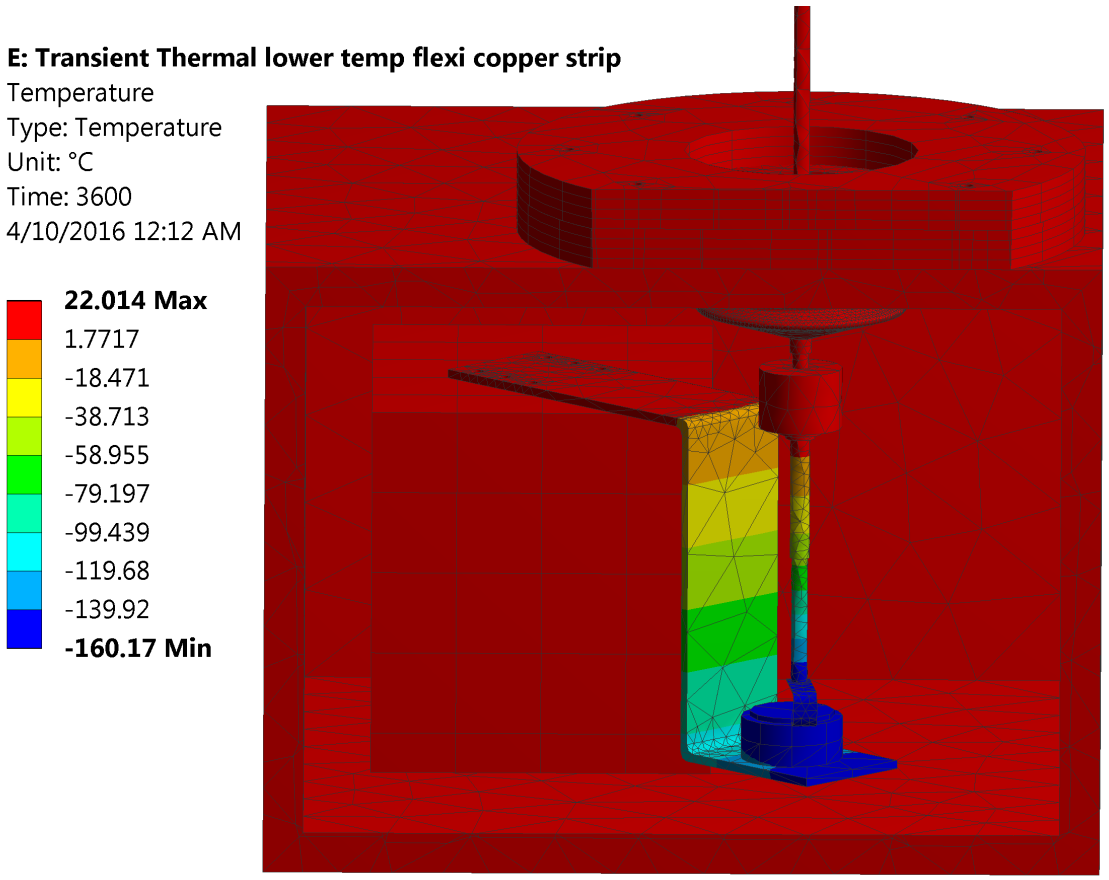

Figure 11: ANSYS thermal simulation output for cooling stage

hole at the end of the copper strip. After that, the model is submitted to simulate output results. Figure 11 shows the ANSYS simulation output for cooling stage and it can be seen from the simulation output that the heat flows toward cooling stage along Z shape bracket. According to heat distribution along Z shape bracket, the top flange of the bracket and connected linear X-Y manual actuators remains at room temperature, unaffected by the extremely low temperature of cooling stage. Also, the indenter part containing load cell remains at room temperature beyond 50mm from indenter tip. It means that any electronic component is safe from the extremely low temperature of cooling stage and indenter tip, beyond 50 mm from indenter tip.

3.4.2 Thermal Analysis for Extreme High Temperature

Similar to thermal analysis for low temperature, thermal analysis for extreme high temperature is carried out. Now the heating stage is set at an extremely high temperature of 120^{o}C, with same end step at 3600 sec. Simulation output for above thermal load is shown in Figure 12. It is clearly observed that the heat flows from electric resistive heating stage along Z shape bracket which is then connected to linear X-Y manual actuators. As shown in Figure 12, the heat distribution because of the electric resistive heating stage, the upper flange of the bracket and linear X-Y manual actuators are at room temperature, unaffected by the extremely high temperature of heating stage. Also, the indenter part and load cell remain at room temperature, beyond 60 mm from indenter tip. Thus, from thermal analysis of extreme temperature it can be concluded that the electronic parts and actuators are in safe limit and remains at room temperature during the experimental measurements.

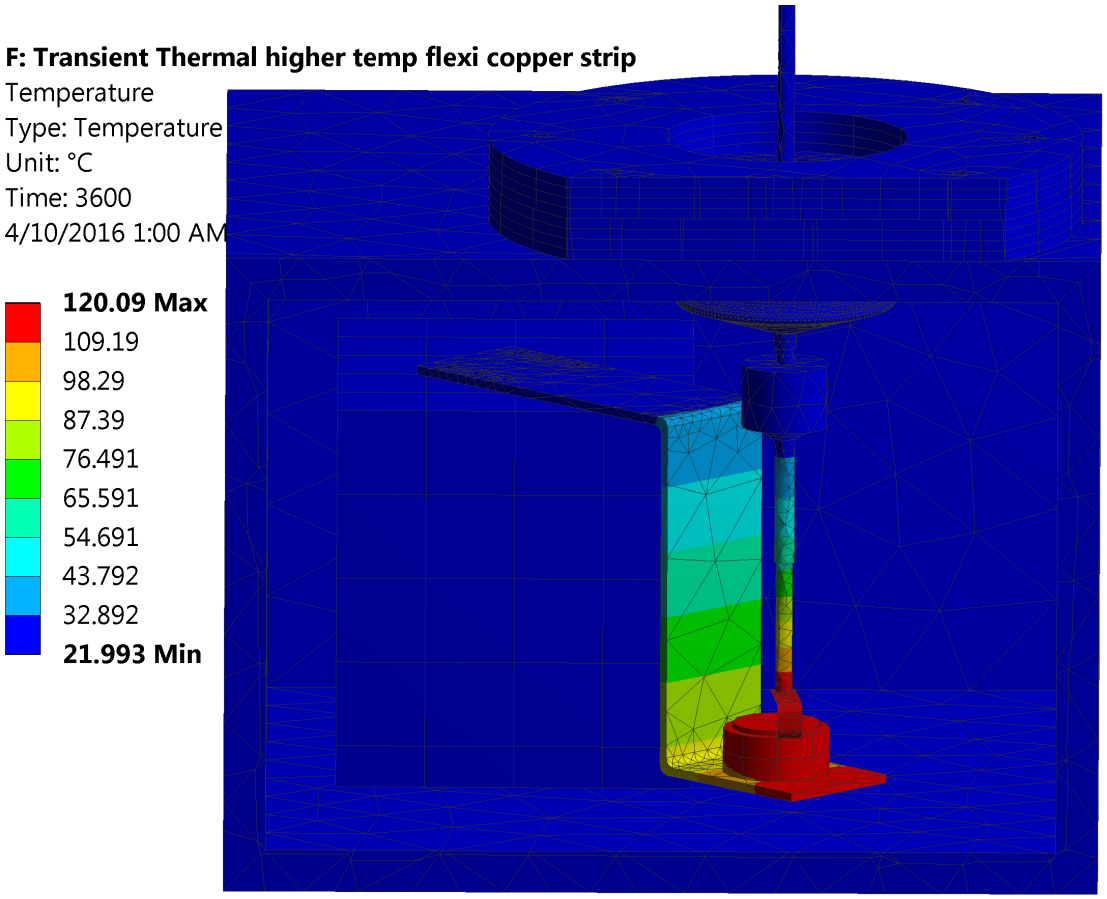

Figure 12: ANSYS thermal simulation output for heating stage

Chapter 4

ADHESION-FRICTION CONTROL SYSTEM

The whole adhesion-Friction testing setup is built in an environment controlled chamber and externally actuated by motorized linear actuators. It consists of the linear X-Y-Z positioning system and a load cell to measure force. Only Z axis positioning linear actuator is used for adhesion test, whereas friction test uses all three X-Y-Z positioning actuators. Prior to experimental measurements of adhesion and friction forces, the sample is aligned using manual alignment stage and applying the alignment process published by Kroner et al,(Kroner *et al.*, 2011).

Entire adhesion-friction testing experiment is controlled by National Instrument's LabVIEW software. MATLAB software file is used as parameter input file to LabVIEW software. Approach velocity, contact time, retracting velocity and final position of indenter are the input parameters to the control system. Except initial calibration of manual linear actuator stage, everything is controlled without manual intervention to avoid any errors.

4.1 LabVIEW Interface to The Control System

The main execution and goals of the code are shown in Figure 13. The main controls involved the combination of Thorlabs APT software for their TDC001 motors (used to control the linear actuators) and LabVIEW itself. In Figure 14 shows the user interfaces for two of the interfaces that have been developed in LabVIEW. The left part of Figure 14 is the user interface for reading the input parameters from a

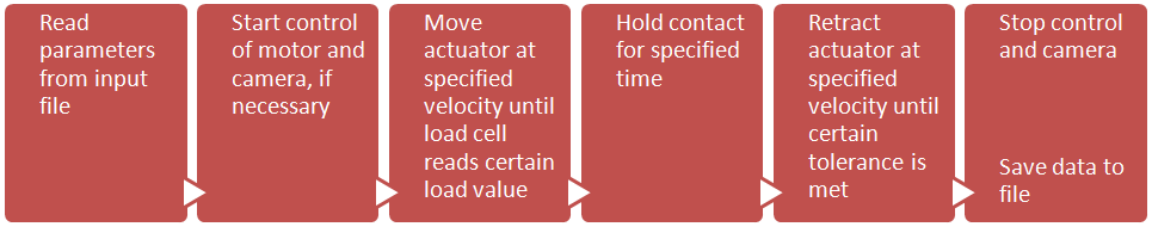

Figure 13: General Pseudo code for how the controls will operate for the adhesion testing with the device

spreadsheet file or MATLAB file. This user interface also includes the option of the user inputting the values directly onto the screen instead of importing the external spreadsheet file. The user is able to select their preference before the code is initiated. The right part of Figure 14 represents the user interface for the testing code that was developed for the main parts of the code (boxes 2-5 in Figure 13).

The input clusters define the min/ max velocity and the acceleration of the device for its approach velocity and its retract velocity. The Boolean switches were used for testing purposes only to simulate the load cell and the tolerance reaching their specified values. The main functionality of the code is based upon "Notifiers", which are often used to control the sequencing of producer/consumer loops in LabVIEW. The switch conditions are used to stop the actuators from moving and also equipped with an "emergency" stop—shown. The emergency switch calculates the maximum time that the actuator can move at its certain velocity and acceleration before it covers enough distance to damage any equipment. This will stop the actuator just in case the load cell or other instruments stop working, saving other instruments from any potential excess damage. Other considerations those are implemented into the final design include a for loop because the experiment will be completed with multiple trials. The code writes all of the data from the multiple trials to a spreadsheet or text

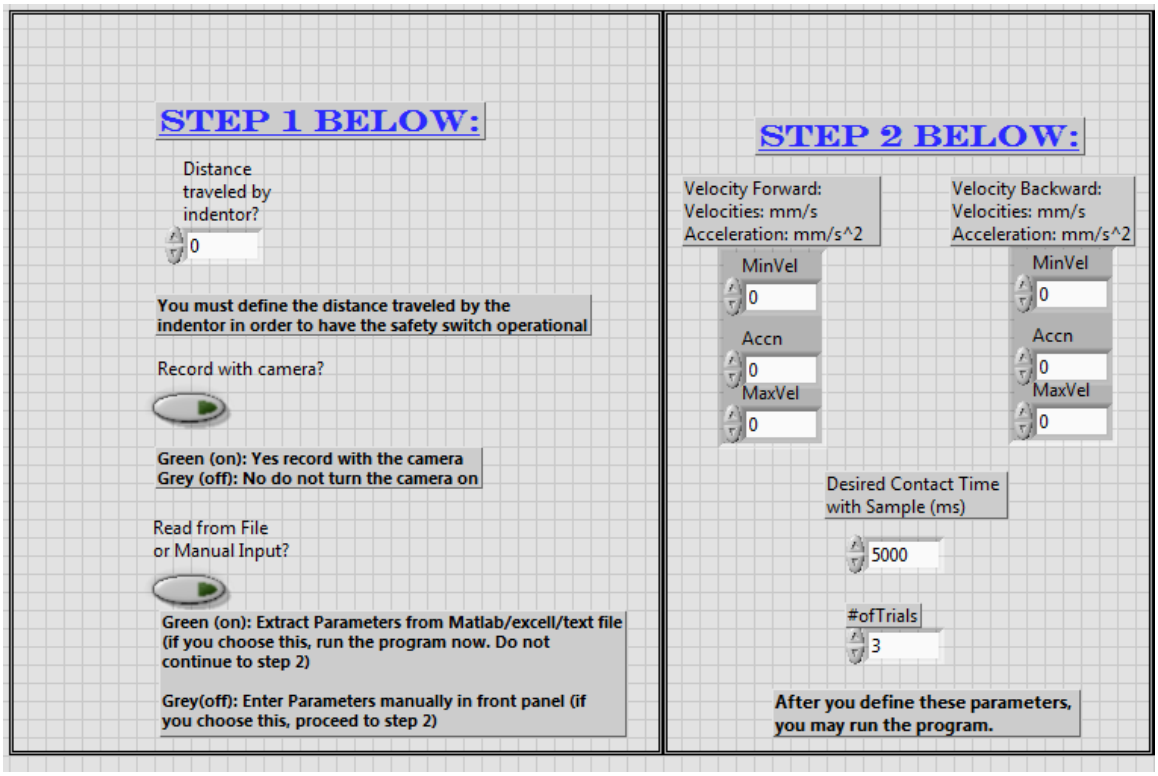

Figure 14: User interfaces of the parameters that will be read from the spreadsheet file

file in order to save all of the data to be analyzed at a later time. The software for the Thorlabs camera is also included in the design. This control turns the camera ON at the beginning of the experiment and off at the end while continuously writing the data to a file.

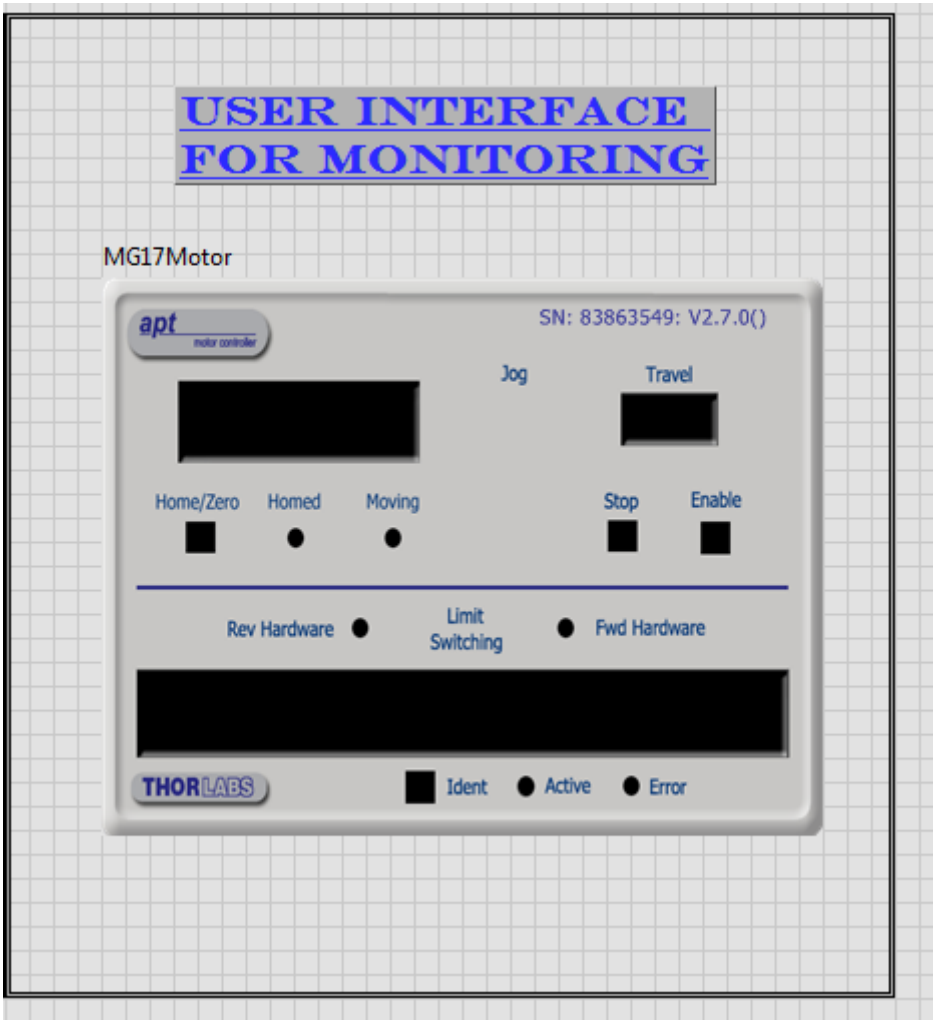

Figure 15: The general user interface for the linear actuator operation

Chapter 5

ADHESION-FRICTION MEASUREMENT

5.1 Adhesion Measurement Procedure in Steps

Before the start of the adhesion measurement, environment conditions in the chamber are maintained by operating vacuum pump and either cryogenic cooling or electric resistive heating system. To obtain an equilibrium surface state, more than 300 contacts were made between a smooth PDMS sample and the glass plate prior to adhesion measurement,(Kroner *et al.*, 2009, 2010). As the desired environmental condition are reached and stabilized inside the chamber, following steps are executed:

Step 1: Compare the pressure and temperature inside the chamber to reference values decided at the start of the experiment. If values are matched then go to next step, otherwise follow sub-steps.

Sub-step 1a: If recorded pressure from the pressure sensor of turbo vacuum pump does not match with the experimental pressure then run the vacuum pump until it matches with experimental pressure value. The in-build PID controller of turbo vacuum pump will take care of maintaining desired pressure inside the chamber.

Sub-step 1b: If recorded temperature from thermopile is greater than experimental temperature value, then run the cryogenic cooling system until temperatures are leveled. If the recorded temperature is less than the experimental temperature then run electric resistive heating system to level up the desired temperature.

Step 2: Read the text file from MATLAB software that specifies parameters such as Approach velocity, contact time, retracting velocity and final position of indenter tip.

Then assign respective values of parameters to the input parameters in the LabVIEW software.

Step 3: Build sub-arrays with the specified parameters in LabVIEW software.

Step 4: Start the camera to record experiment and data collection.

Step 5: Actuate Z-axis motorized linear actuator with specified approach velocity mentioned in Step 1 towards the sample.

Step 6: Stay in contact with the sample for specified contact time and record compression load acting on the sample as indenter moves forward.

Step 7: Retract the indenter from the sample with specified velocity and record the adhesion force measured by load cell during separation of indenter from the sample.

Step 8: Retract the indenter until indenter tip reaches the final position as mentioned in Step 1 and stop camera to record experiment.

5.2 Friction Measurement Procedure in Steps

For friction measurement, the steps are similar to the steps mentioned in the adhesion measurement. Additional Sub-step 6a is included after Step 6. The Sub-step 6a is explained below.

Sub-step 6a: Move the indenter in the X-Y plane, first along the X-axis and then Y-axis. Record the friction force measured by load cell in both directions.

5.3 Experimental Measurement Sets and Analysis

To determine adhesive properties of the sample and its applicability, the following measurement sets and analysis were conducted in the controlled environment. 1)

Controlled environment is maintained at -160^{o}C in the vacuum condition and adhesion force is recorded along with detachment force against time or displacement.

2) Controlled environment is maintained at 120^{o}C in the vacuum condition and adhesion force is recorded along with detachment force against time or displacement.

3) Controlled environment is maintained at a periodic intermediate temperature from -160^{o}C to 120^{o}C in the vacuum condition and adhesion force is recorded along with detachment force against time or displacement.

4) As explained above, the same set of experiment is repeated with different geometry of glass indenter such as a flat face, spherical shape. Also, above experiments repeated with varying geometric parameters of the sample such as active length of the fiber, the geometry of fiber tip and inclination of fibers. Above set of measurements is repeated multiple times to prove their repeatability.

Chapter 6

DESIGN AND FABRICATION OF SWITCHABLE FIBRILLAR STRUCTURES

Depending on the material being used for the fibers as well as their scale and structure, different fabrication techniques could be used, (Marvi *et al.*, 2015a,b; Dhinojwala, 2006; Purtov *et al.*, 2015; Day *et al.*, 2013). Based on the previous finding on robust performance of PDMS adhesive at different environment conditions (pressure, temperature, and humidity), PDMS would be the top choice of material for this experimental study. Polyurethane is another elastomer successfully used for fabricating high-adhesive and robust fibrillar structures (Marvi *et al.*, 2015b; Murphy *et al.*, 2009; Murphy and Sitti, 2007; Aksak *et al.*, 2007) and will be used in this experimental study. The proposed fabrication processes for making fibers using either of these materials at different scales are described in the following:

6.1 Fibers Smaller than 500 Microns in Diameter

A 2D mask will be designed and printed for the fibers and a positive master mold will then be fabricated using lithography techniques. This mold will be made of SU-8, a UV- curable photoresist. Next, a negative mold will be fabricated using a soft silicon rubber. Finally, the positive fibers will be fabricated using PDMS or polyurethane elastomer, (Murphy *et al.*, 2009; Murphy and Sitti, 2007). Any desired tip decoration can then be performed following the procedure reported in the literature (Marvi *et al.*, 2015a).

6.2 Fibers Larger than 500 Microns in Diameter

First, negative mold will be fabricated by drilling holes in acrylic using CNC machine. Next, a positive mold will be fabricated using polyurethane and then a negative mold will be made using a soft silicon rubber. Finally, the positive fibers will be fabricated using PDMS or polyurethane elastomer (Marvi *et al.*, 2015a). Any desired tip decoration can then be performed following the procedures reported in the literature,(Marvi *et al.*, 2015a).

6.3 Proposed Mechanisms for Switching the Adhesive ON/OFF

The Gecko is one of the most memorable participants in nature who utilizes switchable (on/off) adhesive techniques to its advantage. The Gecko moves quickly and conquers many terrains through the use of its switchable adhesive that is defined by: 1) structurally, its hierarchical anisotropic micro and nano structures on the pads of its feet and 2) by the biomechanics of its movement, which consists of the active movements, like shearing or peeling, that the Gecko applies to its foot. Scientists and researchers have been attempting to imitate the Gecko's switchable adhesive technique with many different physical methods. Compressive preloading of a material is one method that grants controllable, switchable adhesion of materials. Purtov, et. all used this pre-loading technique on adhesive pillar structures to initiate reverse buckling, which forced the previously adhesive material to release its contact surface. A maximum buckling preload was determined, both in the air and in a vacuum. If the preload applied to the pillars was less than this maximum, adhesion was "on". As soon

as the maximum preload was surpassed, the adhesion was "off", releasing its contact surface, (Purtov *et al.*, 2015).

Switching capabilities are achieved through a separate method that utilizes the simple principle of the contact area. Jin, et. all used triangular adhesive pillars that gave the fibers preference in gripping direction. When the fibers were pulled (shearing) in the gripping direction, the triangular pillars created a large contact area between itself and the glass surface. When the fibers were pulled the opposite way, a small contact area is formed, causing the fibers to release the glass surface,(Jin *et al.*, 2014). In a separate application, Sariola and Sitti created a combination mesh design to control adhesive capabilities. The base mesh had holes where the pillar structures would extend or retract through. When the pillar structures were extended, the contact area of the surface was increased, resulting in adhesion. When the pillars were retracted, the base mesh was the only thing in contact with the surface. The contact area was decreased, turning the adhesive off,(Sariola and Sitti, 2014). In another application of contact area for adhesive switching, a magnetic field was used. Northen, et. all fabricated cantilever beams that contained nickel. When the magnetic field was applied, the cantilever beams were forced into a different orientation that faced away from the desired contact surface. Not all beams would completely detach from the surface, but the decreased contact area was enough to create the off adhesion switch.

In a final method, Isla, et. all utilizes both of the previously discussed methods. The use of compressive preloading to control contact area was used to create three divisions of adhesive states vs. the traditional two (on or off). This third adhesive division was achieved by adding adhesive pillar structures at two distinct heights. Thus, depending on the compressive preload applied, the number of pillar structures in contact with a surface could be increased or decreased. This method combines

both the idea of compressive preloading and contact area to result in three levels of adhesive switchability, (Isla and Kroner, 2015).

REFERENCES

Aksak, B., M. P. Murphy and M. Sitti, "Adhesion of biologically inspired vertical and angled polymer microfiber arrays", Langmuir **23**, 6, 3322–3332 (2007).

Anitei, S., "A step toward "gecko glue"", URL http://news.softpedia.com/news/A-Step-Toward-Gecko-Glue-74596.shtml (2007).

Arul, E. P. and A. Ghatak, "Control of adhesion via internally pressurized subsurface microchannels", Langmuir **28**, 9, 4339–4345 (2012).

Autumn, K., A. Dittmore, D. Santos, M. Spenko and M. Cutkosky, "Frictional adhesion: a new angle on gecko attachment", Journal of Experimental Biology **209**, 18, 3569–3579 (2006).

Autumn, K., Y. A. Liang, S. T. Hsieh, W. Zesch, W. P. Chan, T. W. Kenny, R. Fearing and R. J. Full, "Adhesive force of a single gecko foot-hair", Nature **405**, 6787, 681–685 (2000).

Autumn, K., M. Sitti, Y. A. Liang, A. M. Peattie, W. R. Hansen, S. Sponberg, T. W. Kenny, R. Fearing, J. N. Israelachvili and R. J. Full, "Evidence for van der waals adhesion in gecko setae", Proceedings of the National Academy of Sciences **99**, 19, 12252–12256 (2002).

Buhl, S., C. Greiner, A. d. Campo and E. Arzt, "Humidity influence on the adhesion of biomimetic fibrillar surfaces", International Journal of Materials Research **100**, 8, 1119–1126 (2009).

Day, P., E. V. Eason, N. Esparza, D. Christensen and M. Cutkosky, "Microwedge machining for the manufacture of directional dry adhesives", Journal of Micro and Nano-Manufacturing **1**, 1, 011001 (2013).

Del Campo, A., C. Greiner and E. Arzt, "Contact shape controls adhesion of bioinspired fibrillar surfaces", Langmuir **23**, 20, 10235–10243 (2007).

Dhinojwala, A., "Synthetic gecko foot-hairs from multiwalled carbon nanotubes", in "APS Meeting Abstracts", (2006).

Feldstein, M. M., K. A. Bovaldinova, E. V. Bermesheva, A. P. Moscalets, E. E. Dormidontova, V. Y. Grinberg and A. R. Khokhlov, "Thermo-switchable pressure-sensitive adhesives based on poly (n-vinyl caprolactam) non-covalently cross-linked by poly (ethylene glycol)", Macromolecules **47**, 16, 5759–5767 (2014).

Gåård, A., N. Hallbäck, P. Krakhmalev and J. Bergström, "Temperature effects on adhesive wear in dry sliding contacts", Wear **268**, 7, 968–975 (2010).

Gorb, S. N., "Biological attachment devices: exploring nature's diversity for biomimetics", Philosophical Transactions of the Royal Society of London A: Mathematical, Physical and Engineering Sciences **366**, 1870, 1557–1574 (2008).

Heepe, L. and S. N. Gorb, "Biologically inspired mushroom-shaped adhesive microstructures", Annual Review of Materials Research **44**, 173–203 (2014).

Henrey, M., J. P. D. Téllez, K. Wormnes, L. Pambaguian and C. Menon, "Towards the use of mushroom-capped dry adhesives in outer space: Effects of low pressure and temperature on adhesion strength", Aerospace Science and Technology **29**, 1, 185–190 (2013).

Hsu, P. Y., L. Ge, X. Li, A. Y. Stark, C. Wesdemiotis, P. H. Niewiarowski and A. Dhinojwala, "Direct evidence of phospholipids in gecko footprints and spatula–substrate contact interface detected using surface-sensitive spectroscopy", Journal of the Royal Society Interface p. rsif20110370 (2011).

Huber, G., S. N. Gorb, N. Hosoda, R. Spolenak and E. Arzt, "Influence of surface roughness on gecko adhesion", Acta Biomaterialia **3**, 4, 607–610 (2007).

Isla, P. Y. and E. Kroner, "A novel bioinspired switchable adhesive with three distinct adhesive states", Advanced functional materials **25**, 16, 2444–2450 (2015).

Jagota, A. and S. J. Bennison, "Mechanics of adhesion through a fibrillar microstructure", Integrative and Comparative Biology **42**, 6, 1140–1145 (2002).

Jeong, H. E., M. K. Kwak and K. Y. Suh, "Stretchable, adhesion-tunable dry adhesive by surface wrinkling", Langmuir **26**, 4, 2223–2226 (2010).

Jiang, H., E. W. Hawkes, V. Arutyunov, J. Tims, C. Fuller, J. P. King, C. Seubert, H. L. Chang, A. Parness and M. R. Cutkosky, "Scaling controllable adhesives to grapple floating objects in space", in "Robotics and Automation (ICRA), 2015 IEEE International Conference on", pp. 2828–2835 (IEEE, 2015).

Jin, K., J. C. Cremaldi, J. S. Erickson, Y. Tian, J. N. Israelachvili and N. S. Pesika, "Biomimetic bidirectional switchable adhesive inspired by the gecko", Advanced Functional Materials **24**, 5, 574–579 (2014).

Kamperman, M., E. Kroner, A. del Campo, R. M. McMeeking and E. Arzt, "Functional adhesive surfaces with "gecko" effect: The concept of contact splitting", Advanced Engineering Materials **12**, 5, 335–348 (2010).

Kier, W. M. and A. M. Smith, "The structure and adhesive mechanism of octopus suckers", Integrative and Comparative Biology **42**, 6, 1146–1153 (2002).

Kim, S., M. Sitti, T. Xie and X. Xiao, "Reversible dry micro-fibrillar adhesives with thermally controllable adhesion", Soft Matter **5**, 19, 3689–3693 (2009).

Kroner, E., R. Maboudian and E. Arzt, "Effect of repeated contact on adhesion measurements involving polydimethylsiloxane structural material", in "IOP Conference Series: Materials Science and Engineering", vol. 5, p. 012004 (IOP Publishing, 2009).

Kroner, E., R. Maboudian and E. Arzt, "Adhesion characteristics of pdms surfaces during repeated pull-off force measurements", Advanced Engineering Materials **12**, 5, 398–404 (2010).

Kroner, E., D. R. Paretkar, R. M. McMeeking and E. Arzt, "Adhesion of flat and structured pdms samples to spherical and flat probes: a comparative study", The Journal of Adhesion **87**, 5, 447–465 (2011).

Loguercio, A., D. Salvalaggio, A. Piva, C. Klein-Júnior, M. de LR Accorinte, M. Meier, R. Grande and A. Reis, "Adhesive temperature: effects on adhesive properties and resin-dentin bond strength", Operative dentistry **36**, 3, 293–303 (2011).

Marvi, H., Y. Han and M. Sitti, "Actively controlled fibrillar friction surfaces", Applied Physics Letters **106**, 5, 051602 (2015a).

Marvi, H., S. Song and M. Sitti, "Experimental investigation of optimal adhesion of mushroomlike elastomer microfibrillar adhesives", Langmuir **31**, 37, 10119–10124 (2015b).

Murphy, M. P., B. Aksak and M. Sitti, "Gecko-inspired directional and controllable adhesion", Small **5**, 2, 170–175 (2009).

Murphy, M. P. and M. Sitti, "Waalbot: An agile small-scale wall-climbing robot utilizing dry elastomer adhesives", Mechatronics, IEEE/ASME Transactions on **12**, 3, 330–338 (2007).

Nadermann, N., J. Ning, A. Jagota and C.-Y. Hui, "Active switching of adhesion in a film-terminated fibrillar structure", Langmuir **26**, 19, 15464–15471 (2010).

Pattantyus-Abraham, A., J. Krahn and C. Menon, "Recent advances in nanostructured biomimetic dry adhesives", Frontiers in bioengineering and biotechnology **1** (2013).

Price, S., T. Phillips and G. Knier, "Staying cool on the iss", Retrieved November **7**, 2010 (2001).

Purtov, J., M. Frensemeier and E. Kroner, "Switchable adhesion in vacuum using bio-inspired dry adhesives", ACS applied materials & interfaces **7**, 43, 24127–24135 (2015).

Ruffatto, D., D. Beganovic, A. Parness and M. Spenko, "Experimental results of a controllable electrostatic/gecko-like adhesive on space materials", in "Aerospace Conference, 2014 IEEE", pp. 1–7 (IEEE, 2014).

Ruibal, R. and V. Ernst, "The structure of the digital setae of lizards", Journal of Morphology **117**, 3, 271–293 (1965).

Russell, A., "A contribution to the functional morphology of the foot of the tokay", (2002).

Sameoto, D. and C. Menon, "Recent advances in the fabrication and adhesion testing of biomimetic dry adhesives", Smart Materials and Structures **19**, 10, 103001 (2010).

Sariola, V. and M. Sitti, "Mechanically switchable elastomeric microfibrillar adhesive surfaces for transfer printing", Advanced Materials Interfaces **1**, 4 (2014).

Wikipedia, "Mean free path — wikipedia, the free encyclopedia", URL https://en.wikipedia.org/w/index.php?title=Mean_free_path&oldid=702246733, [Online; accessed 4-April-2016] (2016).

Zhou, M., N. Pesika, H. Zeng, Y. Tian and J. Israelachvili, "Recent advances in gecko adhesion and friction mechanisms and development of gecko-inspired dry adhesive surfaces", Friction **1**, 2, 114–129 (2013).